

BBReach: Tight and Scalable Black-Box Reachability Analysis of Deep Reinforcement Learning Systems

Jiaxu Tian¹, Dapeng Zhi¹, Si Liu², Peixin Wang³, Guy Katz⁴, and Min Zhang¹

¹ Shanghai Key Laboratory of Trustworthy Computing, ECNU, Shanghai, China

² ETH Zurich

³ University of Oxford

⁴ The Hebrew University of Jerusalem
zhangmin@sei.ecnu.edu.cn

Abstract. Reachability analysis is a promising technique to automatically prove or disprove the reliability and safety of AI-empowered software systems that are developed by using Deep Reinforcement Learning (DRL). Existing approaches suffer however from limited scalability and large overestimation as they must over-approximate the complex and almost inexplicable system components, namely deep neural networks (DNNs). In this paper we propose a novel, tight and scalable reachability analysis approach for DRL systems. By training on abstract states, our approach treats the embedded DNNs as black boxes to avoid the over-approximation for neural networks in computing reachable sets. To tackle the state explosion problem inherent to abstraction-based approaches, we devise a novel adjacent interval aggregation algorithm which balances the growth of abstract states and the overestimation caused by the abstraction. We implement a tool, called BBReach, and assess it on an extensive benchmark of control systems to demonstrate its tightness, scalability, and efficiency.

1 Introduction

Modern AI-empowered software systems such as autonomous driving are typically developed by utilizing Deep Reinforcement Learning (DRL) [29]. In such a system, the well-trained Deep Neural Networks (DNNs) determine the optimal actions during its interactions with the surroundings. Due to the lack of interpretability [11,37] and the vulnerability to adversarial samples [31] for DNNs, concerns have recently been raised about the safety and reliability of DRL [15,26]. Hence, providing provable safety guarantees for DRL systems prior to their deployments is a key challenge for DRL’s application in safety-critical settings.

Reachability analysis, as one of the powerful formal methods, has been applied to the verification of continuous [7] and hybrid [5] systems since the 1990s. To cite a few, its successful applications include invariant checking [24], robust control [20,27], fault detection [28,30], and set-based predication [4,23]. More recently, reachability analysis has been demonstrated to be an effective approach to the verification of DRL systems [10,12,17]. The essence of reachability analysis is to compute all the reachable system states from the given initial state(s). In particular, for a DRL system, one must take every state s from a given set of states, feed s to the planted DNN to determine the corresponding action a on s , and compute the subsequent state s' by applying a to s according to usually nonlinear system dynamics.

Compared to continuous and hybrid systems, it is significantly more challenging to compute reachable states for DRL systems due to the embedded complex and inexplicable DNNs. In addition to over-approximating the nonlinear system dynamics [9,13,21], one also over-approximates the embedded DNNs for computing the reachable states of DRL systems. Specifically, given a set S_i of continuous system states at some step i , one (i) overestimates a set A_i of actions that are applied to S_i by over-approximating the neural network on S_i , and then (ii) overestimates a set of subsequent states by applying A_i to S_i using the over-approximated system dynamics. Such *dual over-approximations* inevitably introduce large overestimation which accumulates step by step, resulting in a considerable number of unreachable states in the computed reachable sets.

Additionally, the state-of-the-art (dual) over-approximation approaches [17,10,12] are also restricted to certain types of neural network architectures and activation functions, as well as the network size [16]. For instance, Verisig 2.0 [17] does not support the neural networks with the ReLU activation functions; Sherlock [10] is applicable only to ReLU-based networks; ReachNN* [12] is not scalable with respect to the network size and more overestimation would be introduced for larger networks.

Our Approach. In this paper we propose a novel, tight and scalable reachability analysis approach for DRL systems. Our approach leverages the recent abstraction-based DRL training method [19], by which the DNN planted in a DRL system can admit an abstract state and produce a unique action. Intuitively, an abstract state represents a (probably infinite) set of actual system states. Given a system state space S and a set of states represented by an interval $I \subseteq S$, our approach proceeds as follows: (i) discretize S into a finite set of abstract states that are represented by interval boxes; (ii) segment I into a set of sub-intervals B_I and feed the abstract state enclosing each interval I in B_I into the neural network to compute the action a ; and (iii) apply action a to I to compute its successor interval I' . The concretization of I' is an over-approximation set of the actual states which are successors from those inside I . This process allows us to treat the DNN as a black-box oracle, which consequently avoids over-approximating it to compute the action for a set of actual states. No over-approximation to the neural network significantly reduces the over-approximation error of computed reachable sets. Moreover, it renders our approach agnostic to the size, the architecture, and the activation function of a neural network.

However, this abstraction-based approach may still suffer from the notorious state-explosion problem with the increasing depth of system transitions. To address this challenge, we propose a novel *adjacent interval aggregation* algorithm to limit the expansion of the number of intervals, thus making the calculation of reachable sets scalable over a longer time horizon. By merging the adjacent intervals, we can significantly restrain the growth in the number of computed intervals, guarantee no much overestimation introduced, and thus reach a balance between the number of intermediate intervals and the overestimation imposed by the aggregation. Moreover, by partitioning the initial set, we enable a parallelizing optimization of our approach that accelerates the problem solving.

Main Contributions. We provide: (i) a novel abstraction-based black-box reachability analysis approach for DRL systems, together with an adjacent interval aggregation algorithm to cope with the state explosion; (ii) an efficient prototype, called BBReach,

with the optimization of parallelizing the computation; and (iii) an extensive assessment of BBReach on a wide range of benchmarks, demonstrating its outperformance over the state-of-the-art tools, the effectiveness of the adjacent interval aggregation algorithm, and the impact of the granularity of the abstractions.

2 Preliminaries

2.1 Deep Reinforcement Learning (DRL)

DRL is a deep-learning-based technique for developing intelligent agents, in which Deep Neural Networks (DNNs) are planted and trained to compute optimal actions on system states. Figure 1 shows the DRL framework. An agent reacts to the environment over time, which is often discretized by a time scale δ [22]. It first observes a state s_t from the environment at each time step t and feeds the state into the network to compute a constant action a_t . Next, the agent transits to the successor state s_{t+1} by performing a_t on s_t according to some environment dynamics and receives a reward r_t from the environment. During training, the process is repeated and the parameters in the network are updated to maximize the cumulative reward. Once the training is completed, the network implements a state-action policy function π that maps each system state to its optimal action. Note that the state space of a DRL system is usually continuous and infinite.

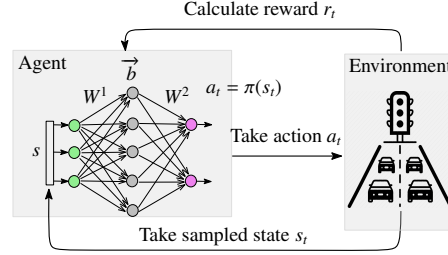


Fig. 1: The DRL framework

Example 1. We consider a classic DRL task of training a two-dimensional agent to move from the initial region $x_1 \in [0.7, 0.9]$ and $x_2 \in [0.7, 0.9]$ to a goal region $x_1 \in [-0.3, 0.1]$ and $x_2 \in [-0.35, 0.5]$. The dynamics f of the environment is defined as follows [14]:

$$x'_1 = x_1 + (x_2 - x_1^3) \cdot \delta \quad x'_2 = x_2 + u \cdot \delta \quad (1)$$

The sign u represents the action to take on x_1, x_2 . Starting from an initial state, the successor state s' is obtained by the dynamics f . If s' is not in the goal region, the agent receives a negative immediate reward, otherwise a positive one. A neural network is trained to guide the agent to the goal region by maximizing the cumulative reward. \square

2.2 Reachability Problem of DRL Systems

We formalize the reachability problem of DRL systems. A trained DRL system can be modeled as a 5-tuple $\mathcal{D} = \langle S, S^0, A, \pi, f \rangle$, where S is the set of n -dimensional system states on n continuous variables, $S^0 \subseteq S$ is the set of initial states, A is the set of system actions, $\pi : S \rightarrow A$ is a policy function implemented by a DNN, and $f : S \times A \rightarrow S$ is a non-linear continuous environment dynamics. \mathcal{D} is essentially a state transition system. A trajectory of \mathcal{D} is defined as a sequence of interleaving states and actions $s_0, a_0, s_1, a_1, s_2, \dots$, where $s_0 \in S^0$ is an initial state. Each action a_t is determined by

current state s_t and neural network π , i.e., $a_t = \pi(s_t)$. Every state s_t ($t > 0$) is determined by environment dynamics f , action a_{t-1} and its preceding state s_{t-1} , i.e., $s_t = f(s_{t-1}, a_{t-1})$. Given two states $s, s' \in S$, there is a one-time step transition from s to s' , denoted by $s \xrightarrow{\pi, f} s'$, if there exists an action a such that $a = \pi(s)$ and $s' = f(s, a)$.

Definition 1 (Reachable state space). Given a trained DRL system $\mathcal{D} = \langle S, S^0, A, \pi, f \rangle$, let $\mathcal{R}_{\mathcal{D}}$ be the least set of all the reachable states such that:

- $S^0 \subseteq \mathcal{R}_{\mathcal{D}}$;
- For all $s, s' \in S$, $s' \in \mathcal{R}_{\mathcal{D}}$ if $s \in \mathcal{R}_{\mathcal{D}}$ and $s \xrightarrow{\pi, f} s'$.

The reachability problem of a DRL system \mathcal{D} is to determine whether an arbitrarily given state s is reachable or not from some state in S^0 . The problem is undecidable in general because the reachability problem of most nonlinear systems are undecidable [6].

Theorem 1 (Undecidability). Given a trained DRL system $\mathcal{D} = \langle S, S^0, A, \pi, f \rangle$ and a state $s \in S$, it is undecidable whether $s \in \mathcal{R}_{\mathcal{D}}$ is true or not.

Definition 2 (t -step reachability). Given a trained DRL system $\mathcal{D} = \langle S, S^0, A, \pi, f \rangle$, a state $s \in S$ and time step t ($t \in \mathbb{Z}^+$), s is t -step reachable if there exists $s' \in S$ such that s' is $(t-1)$ -step reachable and $s = f(s', \pi(s'))$. The states in S^0 are 0-step reachable.

Let $\mathcal{R}_{\mathcal{D}, t}$ be the set of all the t -step reachable states. The bounded reachability problem of \mathcal{D} is to compute $\mathcal{R}_{\mathcal{D}, t}$ for a given time step t . When S^0 is finite, it is straightforward to compute $\mathcal{R}_{\mathcal{D}, t}$ by computing a bounded list of reachable states from each initial state. However, S^0 in DRL is almost always infinite, represented by the intervals for the state variables. The infinity of S^0 makes the problem of computing $\mathcal{R}_{\mathcal{D}, t}$ challenging.

Definition 3 (Reach-Avoid Problem). For a trained DRL system \mathcal{D} , given a set of goal states S_g , a set of unsafe states S_u ($S_g \cap S_u = \emptyset$) and a time horizon T , the reach-avoid problem is to check whether there exists a trajectory $s_0, a_0, s_1, a_1, s_2, \dots, s_T$ of \mathcal{D} such that $\forall 0 \leq t \leq T, s_t \notin S_g$ or $\exists 0 \leq t \leq T, s_t \in S_u$.

The reach-avoid problem is to search for all trajectories and prove \mathcal{D} always reaches a set of goal states and avoids unsafe states within some time horizon T . Through over-approximating $\mathcal{R}_{\mathcal{D}, t}$ for $0 \leq t \leq T$, we can check whether the goal region is eventually reachable and the unsafe region is not reachable. Definition 3 is a variant of the reach-avoid problem defined in [36].

3 Deep Reinforcement Learning with State Abstraction

Over-approximating the reachable states directly on \mathcal{D} is non-trivial as the dual over-approximations are inevitable. In this paper, we try to avoid the over-approximation for the neural network by introducing a specific type of abstraction functions on the basis of \mathcal{D} . Given a system state space S , we denote S_ϕ as a finite set of abstract states (each abstract state represents a possibly infinite set of actual system states in S). Let $\phi : S \rightarrow S_\phi$ be an abstraction function that maps each actual state s in S to

the corresponding abstract state in S_ϕ , and $\tau : S_\phi \rightarrow 2^S$ be the inverse concretization function such that $\tau(s_\phi) = \{s | s \in S, \phi(s) = s_\phi\}$. The basic idea of DRL with state abstraction is to feed the abstract state $\phi(s)$ instead of an actual state s into a neural network to calculate an optimal action. It guarantees that all the actual states in $\tau(s_\phi)$ share a unique action determined by the network [19]. During the training phase, the 4-tuple $(\phi(s_t), a_t, r_t, \phi(s_{t+1}))$ is collected to update the neural network. We call a trained DRL system with state abstraction as an abstract-state based DRL (ASDRL) system.

An ASDRL system can be represented by $\mathcal{M} = (S, S_\phi, A, \pi, f, \phi)$. A trajectory of an ASDRL system is also a sequence of interleaving states and actions $s_0, a_0, s_1, a_1, s_2, \dots$. The only difference from the trajectory of \mathcal{D} is that each action a_t of \mathcal{M} is determined by first applying ϕ to s_t and feeding $\phi(s_t)$ into neural network π , i.e., $a_t = \pi(\phi(s_t))$.

In general, the goal of state abstraction is to reduce the size or complexity of the state space by grouping together similar states [1]. In [19], another significant target of state abstraction is to facilitate the verification of reinforcement learning systems through discretizing the continuous state space S into a finite set of intervals. Specifically, the abstract state space S_ϕ is obtained by dividing each dimension in the original n -dimensional state space into a set of intervals, which means each abstract state can be represented as a $2n$ -dimensional vector $(l_1, u_1, \dots, l_n, u_n)$. We also call the $2n$ -dimensional vector as an interval box.

In what follows, an interval box is used to represent a set of actual states inside its bound. That is, for a $2n$ -dimensional vector $(l_1, u_1, \dots, l_n, u_n)$, we use it to represent the set of n -dimensional actual states $\{(x_1, \dots, x_n) | l_i \leq x_i < u_i, \forall 1 \leq i \leq n\}$. In this work we divide the state space uniformly for better scalability. More specifically, let L_i and U_i be the lower and upper bounds for the i -th dimension value of S . We first define the abstraction granularity as an n -dimensional vector $\gamma = (d_1, d_2, \dots, d_n)$. Then the i -th dimension will be divided evenly into $(U_i - L_i)/d_i$ intervals. With the interval-based discretization, we define the interval-based abstraction function as follows:

Definition 4 (Interval-based Abstraction Function). *Given an n -dimensional continuous state space S and an abstract state space S_ϕ obtained by discretizing S based on an abstraction granularity γ , for every actual state $s = (x_1, \dots, x_n) \in S$ and abstract state $s_\phi = (l_1, u_1, \dots, l_n, u_n) \in S_\phi$, the interval-based abstraction function $\phi : S \rightarrow S_\phi$ is defined as $\phi(s) = s_\phi$ if and only if for each dimension $1 \leq i \leq n : l_i \leq x_i < u_i$.*

Example 2. Consider a simple example in Figure 2, here we have two state variables x_1 and x_2 whose the lower and upper bounds are both 0 and 0.5, respectively. By choosing the abstraction granularity as $(0.1, 0.1)$, we can have the corresponding abstract state $(0.3, 0.4, 0.2, 0.3)$ of an actual state $(0.35, 0.25)$. With an interval-based abstraction function defined above, we can obtain an ASDRL system depicted in Figure 2.

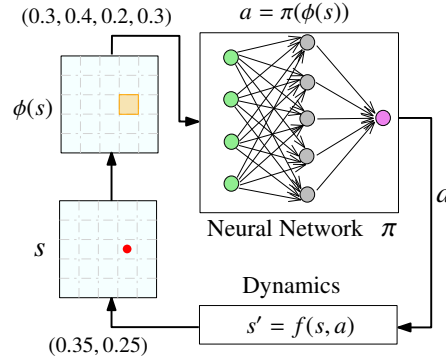


Fig. 2: The ASDRL system

Remark 1. The differences from the general DRL system lie in the interval-based abstraction function and the neural network. The interval-based abstraction function converts the n -dimensional actual state into an abstract state denoted by a $2n$ -dimensional vector. Consequently, the number of neurons in the input layer of the neural network needs to be doubled to make $\phi(s)$ as an input. Such differences ensure that the trained network can produce the same action for all the actual states located in the same interval box.

4 The Abstraction-based Reachability Analysis Approach

In this section we first present the overall process of over-approximating the reachable states of an ASDRL system with the abstraction function specified in Definition 4. We then discuss three techniques, namely interval-based over-approximation, interval segmentation, and adjacent interval aggregation, which are used to achieve efficient calculation and to limit both the increase of computed intermediate intervals and the over-approximation error. The three techniques are all operations defined on interval boxes, which constitute a whole abstract state space.

4.1 Overview of Our Approach

Given an ASDRL system \mathcal{M} and a time horizon T , our reachability analysis aims to compute a sequence of reachable sets $X_0, X_1, X_2, \dots, X_T$ in which $X_{t+1} = \text{aggregate}(\text{post}(X_t))$ for $0 \leq t < T$ to over-approximate the true reachable states of \mathcal{M} . Each reachable set X_t consists of a set of interval boxes enclosing the true reachable states at time step t . The *post* operator computes a set of interval boxes that encloses all reachable states after one time step from a given set of states, while it can also be used to compute the successor state of a given state. In our approach, the *post* operation is executed by formulating it as an optimization problem when the input is an infinite set. However, the formulated optimization problem cannot be directly solved due to the neural network component and abstraction function. To deal with this issue, we present the interval segmentation technique to transform the original optimization problem into several simplified problems. However, interval segmentation will lead to a rapid increase in the number of interval boxes, and hence, we use the *aggregate* operation to limit the expansion of number of interval boxes to make our approach scalable over a longer time horizon.

The overall computation process of reachable sets is presented in Algorithm 1. It is an iterative process where each iteration calculates the reachable set at next time step based on the current reachable set.

Algorithm 1: Reachable sets calculation

Input : ASDRL $\mathcal{M} = (S, S^0, A, \pi, f, \phi)$
Time horizon T

Output : Reachable sets

```

1 Compute an interval  $I_0$  satisfying  $S^0 \subseteq I_0$ 
2  $X_0 = [I_0]$ 
3 for  $t = 1, \dots, T$  do
4   interval_arr = []
5   for  $I$  in  $X_{t-1}$  do
6     segmented_intervals = segment( $I, \phi$ )
7     for  $I$  in segmented_intervals do
8       interval_arr.append( $\text{post}(I)$ )
9    $X_t = \text{aggregate}(\text{interval\_arr})$ 
10 return  $X_0, X_1, \dots, X_T$ 

```

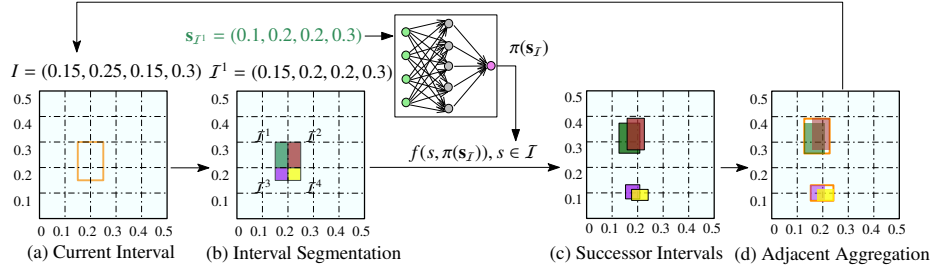


Fig. 3: An example of over-approximating one-step reachable states

Figure 3 depicts the process of one iteration. The abstraction function ϕ depicted by the black dotted mesh in Figure 3 divides the state space into a set of interval boxes (i.e. the smallest black dotted boxes), each of which represents an abstract state. In Figure 3(a), suppose the orange box denotes the reachable set $X_{t-1} = \{I\}$. To compute X_t , we divide I into a set of smaller interval boxes denoted by different colors according to ϕ illustrated in Figure 3(b), which is executed in line 6 of Algorithm 1. Then for each interval box in Figure 3(b), we over-approximate the reachable states from it after one time step in line 8. For instance, through calculating the corresponding abstract state s_{I^1} of interval box I^1 and feed s_{I^1} into the neural network, the action is determined as a constant without any over-approximation error for the neural network π , which renders our approach the black-box feature. After the over-approximation process for the system dynamics f , the over-approximation result $post(X_{t-1})$ including four interval boxes is shown in Figure 3(c). Finally, in line 9 we aggregate the interval boxes adjacent to each other and obtain the larger interval boxes denoted by the orange boxes in Figure 3(d). The aggregation result constitutes the set X_t . Repeating the above process can produce the sequence of reachable sets.

4.2 Over-Approximation of Environmental Dynamics

Given a set of interval boxes X_t , we need to compute $post(X_t)$ by over-approximating the reachable states starting from all interval boxes in X_t after one time step owing to the non-linearity of system dynamics f . By parameterizing the bound of a reachable set, one can solve an optimization problem minimizing or maximizing a specific metric under the constraint that all solutions have to be enclosed [3].

Interval-Based Over-Approximation. Therefore, we formulate the calculation of $post(X_t)$ as optimization problems defined on each interval box in X_t . Specifically, for each interval box I_{X_t} in X_t , we can compute the upper and lower bounds of $post(I_{X_t})$ for each dimension i by solving the following two optimization problems respectively:

$$\arg \max_{s_t \in I_{X_t}} v_i \cdot f(s_t, \pi(\phi(s_t))) \quad \arg \min_{s_t \in I_{X_t}} v_i \cdot f(s_t, \pi(\phi(s_t))) \quad (2)$$

where v_i is a one-hot vector with only the i -th element being 1 and the value of other elements are 0. Based on the above computation, we can obtain the reachable set after one time step as $post(X_t) = \bigcup_{I_{X_t} \in X_t} post(I_{X_t})$. However, the difficulty in these optimization problems is that the objective function $v_i \cdot f(s_t, \pi(\phi(s_t)))$ is non-differentiable and discontinuous, which implies that these optimization problems cannot be solved directly.

Interval Segmentation. As noted above, we compute the reachable sets by solving the optimization problems in expression (2). However, notice that in these optimization problems, $\pi(\phi(s_t))$ is related to both the neural network controller and the abstraction function which means $\pi(\phi(s_t))$ may not be a continuous and differentiable function. To tackle this problem, we propose to use interval segmentation: divide each interval box I_{X_t} in X_t based on abstraction function ϕ .

Based on the abstraction function we defined, the continuous state space is divided into a set of abstract states S_ϕ in which each abstract state is an interval box. Each interval box I_{X_t} may intersect with multiple abstract states. Considering that the neural network outputs the same action on the actual states corresponding to a same abstract state, we segment I_{X_t} into a set of sub-intervals in which all the actual states within the same sub-interval correspond to a same abstract state as depicted in Figure 4. Specifically, we define $\mathbf{S}_{I_{X_t}} = \{s_\phi \mid s_\phi \cap I_{X_t} \neq \emptyset\}$ as the set of abstract states that intersect with the interval box I_{X_t} firstly. Based on the abstraction function, we divide I_{X_t} into a set of interval boxes $\mathbf{B}_{I_{X_t}} = \{I_{X_t} \mid I_{X_t} = s_\phi \cap I_{X_t} \wedge s_\phi \in \mathbf{S}_{I_{X_t}}\}$. Thereafter, for each interval box I_{X_t} in $\mathbf{B}_{I_{X_t}}$, we can solve the following optimization problems:

$$\arg \max_{s_t \in I_{X_t}} v_i \cdot f(s_t, \pi(\phi(s_t))) \quad \arg \min_{s_t \in I_{X_t}} v_i \cdot f(s_t, \pi(\phi(s_t))) \quad (3)$$

For every interval box $I_{X_t} \in \mathbf{B}_{I_{X_t}}$, we have $\forall s'_1, s'_2 \in I_{X_t} : \phi(s'_1) = \phi(s'_2)$. Therefore, in these two optimization problems, $\pi(\phi(s_t))$ can be replaced by a constant which makes these optimization problems easy to be solved. This segmentation process makes the original optimization problems defined on I_{X_t} converted to $|\mathbf{B}_{I_{X_t}}|$ easy-to-solve optimization problems, which implies $post(I_{X_t}) = \{post(I_{X_t}) \mid I_{X_t} \in \mathbf{B}_{I_{X_t}}\}$.

4.3 Adjacent Interval Aggregation

Since the interval segmentation obtains $|\mathbf{B}_{I_{X_t}}|$ interval boxes for each interval box I_{X_t} in X_t , the number of interval boxes will increase rapidly with the increase of time step t , which makes the computation of reachable sets extremely time-consuming. For this reason, we need to use the *aggregate* operation which combines multiple interval boxes into their minimum bounding rectangle to reduce the number of interval boxes.

Figure 5 illustrates this aggregation process. Supposing X_t contains only one interval box, through the interval segmentation and interval-based over-approximation, we will obtain four interval boxes in $post(X_t)$ depicted in Figure 5a. If we skip the aggregation procedure and proceed directly to the calculation at next time step, X_{t+1} will consist of four interval boxes in Figure 5b. This will lead to an exponential growth rate of the number of interval boxes with the increase of time step t . On the contrary, if all the interval boxes in $post(X_t)$ are directly aggregated into one interval box, there will produce large over-approximation error after aggregation as illustrated in Figure 5d. Therefore, to ensure the efficiency of the calculation without introducing large overestimation, we need to find adjacent interval boxes and aggregate them displayed in Figure 5c.

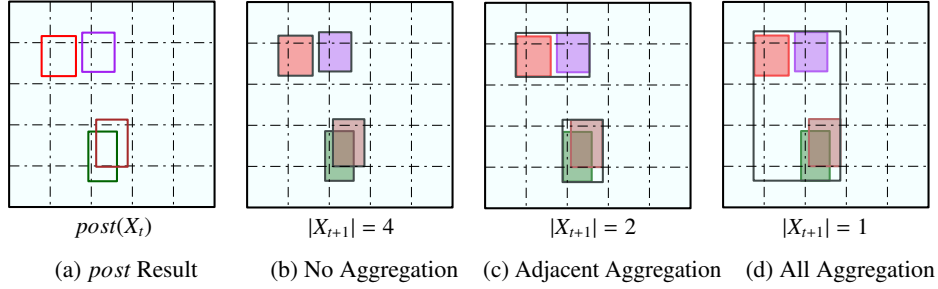


Fig. 5: The effect of adjacent interval aggregation.

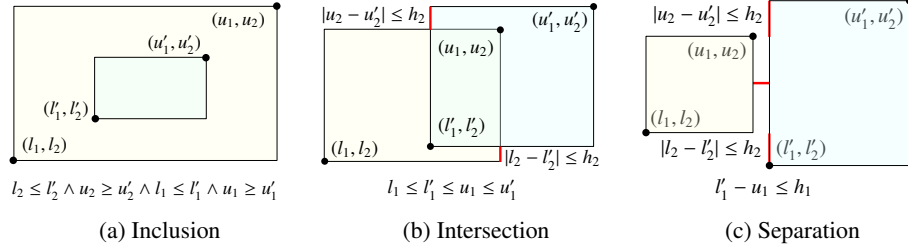


Fig. 6: Visualizing the adjacent relation.

Adjacent Relation. To perform the adjacent interval aggregation, we need to define the adjacent relation initially. In this paper, we define the adjacent relation between interval boxes $A = (l_1, u_1, \dots, l_n, u_n)$ and $B = (l'_1, u'_1, \dots, l'_n, u'_n)$ as the following three forms in which $h = (h_1, \dots, h_n)$ is the preset distance threshold. At first, for the case where one interval box is completely included in the other interval box, we need to aggregate them to avoid repetitive calculation. Then the intersection relation is defined to aggregate those interval boxes that have intersection and would not induce large over-approximation error after aggregation. The separation relation is similar to the intersection one but two interval boxes do not intersect. Figure 6 illustrates the following three forms.

1. Inclusion Relation:

$$\forall i \in \mathbb{N}, 1 \leq i \leq n : (l_i \leq l'_i \wedge u_i \geq u'_i) \vee (l_i \geq l'_i \wedge u_i \leq u'_i)$$

2. Intersection Relation:

$$\exists! d \in \mathbb{N}, 1 \leq d \leq n : l'_d \leq l_d \leq u'_d \leq u_d \vee l_d \leq l'_d \leq u_d \leq u'_d;$$

$$\forall i \in \mathbb{N}, i \neq d \wedge 1 \leq i \leq n : |l_i - l'_i| \leq h_i \wedge |u_i - u'_i| \leq h_i$$

3. Separation Relation:

$$\exists! d \in \mathbb{N}, 1 \leq d \leq n : l_d - u'_d \leq h_d \vee l'_d - u_d \leq h_d;$$

$$\forall i \in \mathbb{N}, i \neq d \wedge 1 \leq i \leq n : |l_i - l'_i| \leq h_i \wedge |u_i - u'_i| \leq h_i$$

With the definition of adjacent relation, for the adjacent interval aggregation problem, a brute-force algorithm is to check and aggregate two adjacent interval boxes by traversing all interval boxes repeatedly until no interval boxes can be aggregated together. The time complexity of traversing n interval boxes once to detect the existence of adjacent relation is $O(n^2)$. In the worst case, it requires traversing n times. Hence, the time complexity of this algorithm is $O(n^3)$.

To achieve the adjacent interval aggregation more efficiently, we propose a novel algorithm shown in Algorithm 2. The key idea is to assume that the adjacent relation is transitive. For instance, if interval box A is adjacent to interval box B and B is adjacent to interval box C , then the interval boxes A, B, C can be aggregated together in our algorithm. Based on this assumption, we pre-construct an adjacency matrix to store the adjacent relations between the interval boxes in $post(X_t)$ firstly. This procedure is executed at line 2 in Algorithm 2 with the time complexity $O(n^2)$. We then implement this adjacent interval aggregation procedure using breadth-first search with the time complexity $O(n^2)$. Hence, the holistic time complexity is optimized to $O(n^2)$.

Algorithm 2: Adjacent Interval Aggregation

Input : The interval boxes set $post(X_t)$
Output : The aggregation results Arr

```

1 Initialize flag = [False, False,...],  $Arr = []$ 
2 Construct the adjacency matrix  $M$ 
3 for  $I_p$  in  $post(X_t)$  do
4   if not flag[ $I_p$ ] then
5     Initialize queue = [ $I_p$ ]
6     while queue is not empty do
7        $I = \text{queue.pop}()$ 
8       flag[ $I$ ] = True
9        $I_{adj} = \text{getAdjacent}(I, M)$ 
10      for item in  $I_{adj}$  do
11         $I_p = \text{aggInterval}(I_p, \text{item})$ 
12        if not flag[item] then
13          queue.put(item)
14       $Arr.add(I_p)$ 
15 return  $Arr$ 

```

Example 3. Consider the two-dimensional system in Example 1. Supposing the $post(X_t)$ includes four interval boxes: $\hat{I}_1 = (0.08, 0.16, 0.3, 0.4)$, $\hat{I}_2 = (0.17, 0.25, 0.32, 0.42)$, $\hat{I}_3 = (0.19, 0.27, 0.07, 0.2)$, $\hat{I}_4 = (0.2, 0.28, 0.1, 0.21)$ and the distance threshold is $h = (0.02, 0.02)$, according to the definition of adjacent relation, we can conclude that \hat{I}_1, \hat{I}_2 have separation relation and \hat{I}_3, \hat{I}_4 have intersection relation. Thus, after adjacent interval aggregation, we obtain a set of two interval boxes $X_{t+1} = \{I_{1,2} = (0.08, 0.25, 0.3, 0.42), I_{3,4} = (0.19, 0.28, 0.07, 0.21)\}$.

4.4 The Soundness

Our reachability analysis approach consists of the $post$ operation defined on each interval box generated from the interval segmentation, and the adjacent interval aggregation process. Lemma 1 proves the soundness of $post$ operation defined on each interval box in $B_{I_{X_t}}$. The soundness guarantee of adjacent interval aggregation is given in lemma 2.

Lemma 1. For each interval box $I \in B_{I_{X_t}}$, we have $s_{t+1} \in post(I)$ for $\forall s_t \in I$.

Proof. $post(I)$ is an interval box that contains a set of states and $s_{t+1} = post(s_t)$. Then we need to prove that for each dimension i , the i -dimensional value of $post(s_t)$ is included in the i -dimensional interval of $post(I)$. According to the optimization problems in expression 3. For each dimension i , we calculate the lower bound l_i and upper bound u_i of $v_i \cdot f(s, \pi(\phi(s)))$ defined on I . Due to $s_t \in I$, we have $\forall s \in I, \pi(\phi(s)) = \pi(\phi(s_t)) = a$ where a is a constant, and for an arbitrary dimension i we obtain:

$$l_i = \min_{s \in I} v_i \cdot f(s, a) \leq v_i \cdot post(s_t) = v_i \cdot f(s_t, a) \leq \max_{s \in I} v_i \cdot f(s, a) = u_i.$$

It now follows that $s_{t+1} = post(s_t) \in post(I)$. □

Lemma 2. Given a set of interval boxes X , let Arr denote the adjacent interval aggregation result of X . We have $\forall I \in X, \exists \hat{I} \in Arr : I \subseteq \hat{I}$.

Proof. In algorithm 2, every interval box in X needs to be traversed. For each interval box $I \in X$, there exist two cases: (i) I is not involved in the adjacent interval aggregation process,. In this case, I will be directly added to Arr , thus $\exists \widehat{I} = I : I \subseteq \widehat{I}$. (ii) I is aggregated into another interval box I' . Since the *aggregate* operation produces the minimum bounding rectangle which encloses all interval boxes involved, we have $\exists \widehat{I} = I' : I \subseteq \widehat{I}$. Consequently, we conclude that $\forall I \in X, \exists \widehat{I} : I \subseteq \widehat{I} \wedge \widehat{I} \in Arr$. \square

The following theorem establishes the soundness of our reachability analysis approach, i.e., all true reachable states are contained in the reachable sets we computed.

Theorem 2. *Given an ASDRL system $\mathcal{M} = (S, S^0, A, \pi, f, \phi)$, for every trajectory $s_0, a_0, s_1, a_1, \dots$ where $s_0 \in S^0$ and the sequence of computed reachable sets X_0, X_1, X_2, \dots with $X_0 = \{I_{X_0}\} \wedge S^0 \subseteq I_{X_0}^1$, we have $\forall t \in \mathbb{N}$, there exists an interval box $I, s_t \in I \wedge I \in X_t$.*

Proof. By induction on the length of trajectories. Given an arbitrary trajectory $s_0, a_0, s_1, a_1, \dots$, we have:

Base Case: $t = 0$: Since $s_0 \in S^0$ and $S^0 \subseteq I_{X_0}$, we have $s_0 \in I_{X_0} \wedge I_{X_0} \in X_0$.

Induction Step: $t \in \mathbb{Z}^+$: Assume $s_t \in I_{X_t}^{n_1} \wedge I_{X_t}^{n_1} \in X_t$ holds. Then, we just need to prove there exists an interval box I satisfying $s_{t+1} \in I \wedge I \in X_{t+1}$. Firstly, let us consider the segmentation process for $I_{X_t}^{n_1}$, we divide $I_{X_t}^{n_1}$ into a set of interval boxes $\mathbf{B}_{I_{X_t}^{n_1}} = \{I_{X_t}^1, I_{X_t}^2, \dots, I_{X_t}^{max}\}$ with $I_{X_t}^{n_1} = \bigcup_{n=1}^{max} I_{X_t}^n$. Thus $\exists n_2 \in \mathbb{Z}^+ : s_t \in I_{X_t}^{n_2}$. Based on Lemma 1, we have $s_{t+1} = post(s_t) \in post(I_{X_t}^{n_2})$. After the adjacent interval aggregation process, X_{t+1} consists of the aggregation result. According to Lemma 2, we have $\exists \widehat{I} : post(I_{X_t}^{n_2}) \subseteq \widehat{I} \wedge \widehat{I} \in X_{t+1}$. Therefore, we have $s_{t+1} \in \widehat{I} \wedge \widehat{I} \in X_{t+1}$ and we can conclude that $\forall t \in \mathbb{N}$, there exists an interval box I such that $s_t \in I \wedge I \in X_t$ for every trajectory. \square

5 Experiments

In this section we conduct a comprehensive assessment of BBReach and the state-of-the-art tools. Our goal is mainly threefold: to demonstrate (i) BBReach’s high scalability and efficiency (Section 5.2), (ii) its tightness with respect to verification results (Section 5.3), and (iii) the effectiveness of the adjacent interval aggregation (Section 5.4). Additionally, we evaluate how BBReach performs under different abstraction granularity levels (Section 5.4).

5.1 Implementation and Benchmarks

Implementation. We implement our approach in a tool called BBReach in Python. We use the SciPy [35] package as an optimization solver. Additionally, we employ the parallelized computing by initial-set partition [8], a standard approach used in the reachability analysis of hybrid systems to obtain tighter bounds of true reachable states. With the initial set partitioned into k subsets, the k sub-problems can be solved in parallel, which accelerates our approach with multiple cores.

Competitors. We compare our tool with the state-of-the-art tools, namely Verisig 2.0 [17], which is an approach based on Taylor model propagation, and ReachNN* [12], which approximates neural networks through polynomial regression.

Benchmarks and Properties. The selected benchmarks include 7 reinforcement learning tasks with dimensions ranging from 2 to 6 from Verisig 2.0. For each task, we train four neural networks with different activation functions and the size of neurons and consequently obtain 28 instants totally. It is worth mentioning that for each instant, the weights in the network used for BBReach are different from those for Verisig 2.0 and ReachNN* due to the abstract training approach. Nevertheless, we guarantee that all the trained systems can achieve the best rewards for the same task. In particular, we initialize the neural networks with smaller weights as otherwise Verisig 2.0 would introduce larger over-approximations (see our observations in Appendix A). We also train the networks under different abstraction granularity levels to evaluate how the abstraction granularity affects the efficiency of BBReach.

We set a reach-avoid problem for each task by specifying its goal region and unsafe region. The detailed settings are given in Table 2, Appendix B.

Experimental Setup. All experiments are conducted on a workstation running Ubuntu 18.04 with 32 cores AMD Ryzen Threadripper CPU @ 3.7GHz and 128GB RAM.

5.2 Comparison on Scalability and Efficiency

The verification results and time costs (in seconds) are shown in Table 1. It is observed that our approach succeeds in verifying all 28 instants with any neural network configuration. Verisig 2.0 succeeds in 12 instants, and ReachNN* in 13 instants. The two tools report 1 and 11 unknown cases (marked by Unk), respectively. The unknown cases occur the tools cannot compute a set of reachable states that are completely covered by the goal region. These cases can be verified by BBReach, which means that our approach introduces less over-approximations than the other two tools. Particularly in Tora case, the two tools did not finish calculating the complete reachable sets (marked by DNF) due to the huge over-approximation error. In ACC, the process of ReachNN* was killed due to the memory limitation when processing larger neural networks (4×100). Note that Verisig 2.0 is not applicable to the systems driven by ReLU neural networks, and we mark the corresponding results by N/A.

Regarding efficiency, our approach costs the least time when parallelization is enabled. Even for single core computation, it takes less time than Verisig 2.0 and ReachNN* in most cases. The advantage of verification time becomes more notable when dealing with larger networks. Because we treat the neural network as a black-box mapping instead of over-approximating it layer by layer, the verification time of BBReach with larger neural networks is about the same as the smaller neural networks, or even less. However, the verification time of Verisig 2.0 and ReachNN* both increases significantly in most cases when dealing with larger neural networks.

Based on the above analysis, BBReach demonstrates substantial improvement over Verisig 2.0 and ReachNN* with respect to computation efficiency. Furthermore, BBReach scales well with the size of the neural network controller.

5.3 Comparison on the Tightness

We compare the tightness of the over-approximation results of true reachable states by plotting the reachable sets computed by different methods and the corresponding simulation trajectories. We present the results of B1, B2 and Tora computed by different

Table 1: Comparison on verification time (s) and result (verified or not).

Task	Dim	Network	BBReach			Verisig 2.0			ReachNN*	
			1 core	20 cores	VR	1 core	20 cores	VR	Default	VR
B1	2	Tanh(2×20)	36.0	2.17	✓	45	38	✓	60	Unk
		Tanh(3×100)	40.7	2.34	✓	413	125	✓	162	✓
		ReLU(2×20)	34.1	2.25	✓	—	—	N/A	20	✓
		ReLU(3×100)	105.4	6.56	✓	—	—	N/A	330	Unk
B2	2	Tanh(2×20)	1.0	0.33	✓	5.2	4.1	Unk	71	Unk
		Tanh(3×100)	1.3	0.43	✓	195	49	✓	172	Unk
		ReLU(2×20)	3.5	1.04	✓	—	—	N/A	4	✓
		ReLU(3×100)	5.2	1.44	✓	—	—	N/A	6647	Unk
B3	2	Tanh(2×20)	10.2	0.94	✓	36	28	✓	115	✓
		Tanh(3×100)	10.3	0.94	✓	394	102	✓	93	✓
		ReLU(2×20)	10.1	0.95	✓	—	—	N/A	69	✓
		ReLU(3×100)	0.9	0.14	✓	—	—	N/A	10321	Unk
B4	3	Tanh(2×20)	0.8	0.35	✓	7	5.1	✓	17	✓
		Tanh(3×100)	1.0	0.44	✓	209	35	✓	20	✓
		ReLU(2×20)	1.0	0.44	✓	—	—	N/A	7	✓
		ReLU(3×100)	0.5	0.24	✓	—	—	N/A	18	✓
B5	3	Tanh(3×100)	14.8	0.95	✓	157	44	✓	27	Unk
		Tanh(4×200)	9.6	0.67	✓	2264	232	✓	2344	Unk
		ReLU(3×100)	9.9	0.64	✓	—	—	N/A	90	✓
		ReLU(4×200)	9.7	0.76	✓	—	—	N/A	2845	Unk
Tora	4	Tanh(3×20)	814.3	44.25	✓	69	46	✓	1610	✓
		Tanh(4×100)	843.9	46.17	✓	—	—	DNF	—	DNF
		ReLU(3×20)	230.2	14.11	✓	—	—	N/A	778	✓
		ReLU(4×100)	257.1	14.72	✓	—	—	N/A	—	DNF
ACC	6	Tanh(3×20)	1.7	0.38	✓	113	50	✓	5498	Unk
		Tanh(4×100)	1.8	0.38	✓	3304	410	✓	—	DNF
		ReLU(3×20)	2.0	0.42	✓	—	—	N/A	4633	Unk
		ReLU(4×100)	2.0	0.48	✓	—	—	N/A	—	DNF

Remarks. VR: verification result; Tanh/ReLU($n \times k$): a neural network with the activation function Tanh/ReLU, n hidden layers, and k neurons per hidden layer; N/A: not applicable; ✓: the reach-avoid problem is successfully verified; Unk: the reach-avoid problem could not be verified due to large over-approximation error; DNF: the calculation did not finish; —: no time data available due to N/A or DNF.

methods when dealing with larger neural networks with the Tanh activation functions in Figure 7. The results for the other benchmarks are given in Appendix C.

In Figure 7, the red boxes represent the reachable sets calculated by different methods at each time step. The green lines are the simulation trajectories and the blue box denotes the preset goal region. If there exists a red box completely inside the blue box and all red boxes disjoint from the purple box, the verification succeeds. The more overlap between the green trajectories and the red boxes indicates the more accurate calculation of the reachable sets. In most scenarios, our approach achieves comparable results to Verisig 2.0 and ReachNN*, such as B1, B3, B4, and B5 (we defer the comparison results for B3, B4, and B5 to Appendix C). Regarding B2, our approach performs better than ReachNN* but worse than Verisig 2.0. This is due to the large variation in the decisions made by the corresponding neural networks. As depicted by the simulation trajectories in Figure 7, the agent enters the goal region from different directions, i.e., bottom for the system

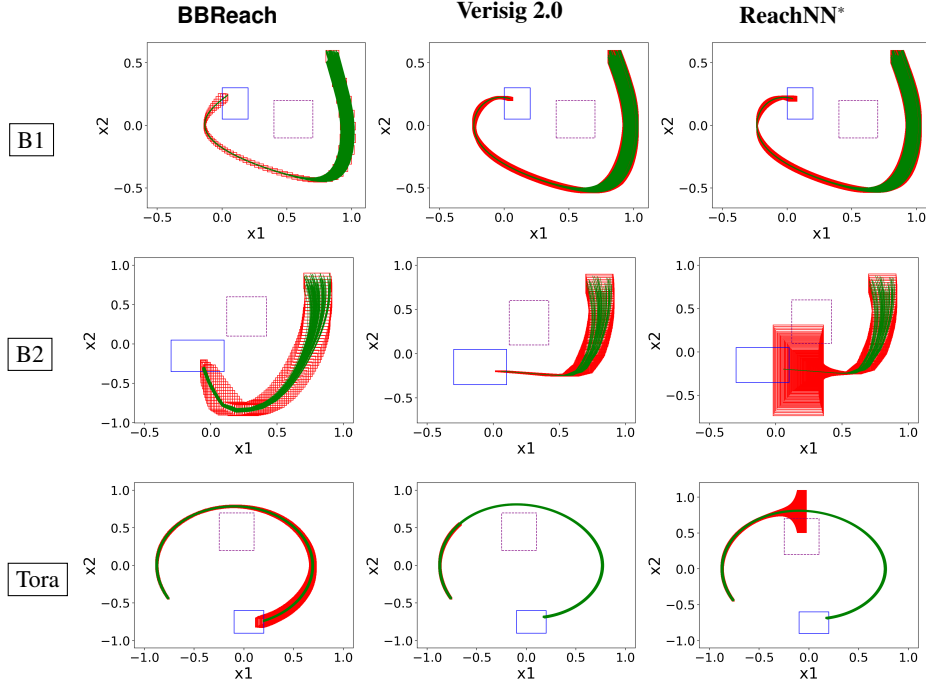


Fig. 7: Larger network with the Tanh activation function. Red box: reachable set; Green lines: simulation trajectories; Blue box: goal region; Purple dashed box: unsafe region.

experimented by BBRach and right for the other one. In this case, BBRach and Verisig 2.0 successfully verified the eventual reachability of the goal region while ReachNN* failed. For Tora, our approach significantly surpasses the competitors: both Verisig 2.0 and ReachNN* did not finish the calculation due to the large over-approximation error. In particular, the resulting bound of action, upon Verisig 2.0’s termination, is $(-95046891, 95048286)$ which is too large for Verisig 2.0 to continue the calculation.

In summary, our approach BBRach is more stable with no huge over-approximation error as in Tora and sufficiently tight to verify all the properties.

5.4 Differential and Decomposing Analysis

Differential Analysis. To demonstrate the significance of the adjacent interval aggregation in Algorithm 2, we measure the growth rate of the number of interval boxes also with no aggregation. Figure 8 shows the results on the B1 benchmark. We observe that the number of interval boxes grows rapidly with no aggregation, which implies a dramatically increased verification overhead. With the adjacent interval aggregation, the number of interval boxes is extremely small and stable. Hence, it is fair to conclude that the adjacent interval aggregation is a substantial benefit to BBRach. The results on the other six benchmarks are similar and provided in Appendix D.

Decomposing Analysis. We evaluate how different abstraction granularity levels affect the performance of BBRach and its components. Abstraction granularity is a crucial

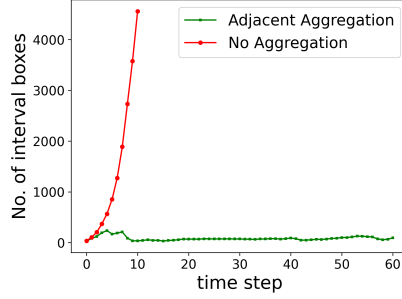


Fig. 8: Differential Analysis on B1

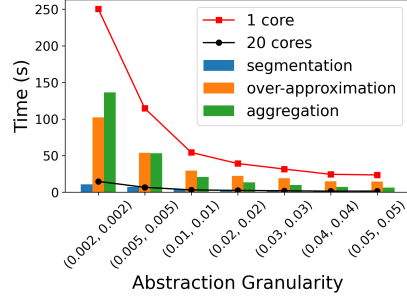


Fig. 9: Decomposing analysis on B1 (Tanh)

hyper-parameter used in both training and calculation of reachable sets. To better understand the impact of abstraction granularity, for each benchmark, in addition to the abstraction granularity level in Table 2, we choose three finer abstraction granularity levels and three coarser abstraction granularity levels, respectively, to evaluate the efficiency on both tanh and relu neural networks. We also measure the time consumed by each of the three steps, i.e., interval segmentation, interval-based over-approximation, and adjacent interval aggregation.

For illustration, we present in Figure 9 the results for B1 with the tanh neural network. Regarding the 1-core results, we observe that, as the abstraction granularity becomes coarse-grained, the verification time decreases and eventually stabilizes; on the other hand, a fairly fine-grained abstraction granularity, e.g., (0.002, 0.002), could result in much higher verification overhead. We also observe that the interval-based over-approximation and the adjacent interval aggregation take most of the verification time while the overhead of the interval segmentation is negligible. Finally, as expected, the parallelization (with 20 cores) can significantly accelerate BBReach. The evaluation results are similar as in the other six cases, which we enclose in Appendix D.

6 Related Work and Conclusion

Many reachability analysis approaches have been developed for DRL systems. Most of them are focused on reducing the overestimation that is caused by the over-approximation of the embedded neural networks. Tran *et al.* [33,34] proposed an approach called NNV by directly combining the star set analysis technique [32] used to deal with the neural network with CORA [2], a reachability analysis tool for non-linear systems. This approach produces large over-approximation error since it omits the dependencies between the neural network inputs and outputs.

To obtain tighter reachable sets, a number of methods have been proposed to capture the input-output relation of neural networks recently. One class of these methods is based on set propagation. Ivanov *et al.* [18,17] proposed a method (i.e., Verisig and Verisig 2.0) that propagates Taylor models layer by layer through the neural network to over-approximate the input-output relation. Schilling *et al.* [25] utilized the zonotope propagation technique to analyze the neural network and presented a method for inter-conversion of zonotope and Taylor model, enabling the combination of the reachability tools used for neural networks and dynamical systems.

Another class of methods tries to approximate a neural network as a whole directly. Huang *et al.* [16,12] proposed an approach (i.e., ReachNN and ReachNN*) to abstract the neural networks with differentiable or non-differentiable activation functions through Bernstein polynomials. Dutta *et al.* [10] proposed Sherlock based on rule generation to compute a polynomial approximation that abstracts the neural network with ReLU activation functions. Because these methods need to sample from the input space of the neural network, it becomes inefficient when handling high-dimensional environments.

We have presented **BBReach**, a tight and scalable abstraction-based reachability analysis approach for DRL systems. **BBReach** leverages the state-of-the-art training technique for neural networks with state abstraction and efficiently computes tight reachable sets with our proposed adjacent interval aggregation to avoid the over-approximation for neural networks. We have experimentally demonstrated that **BBReach** is compatible to neural networks with arbitrary activation functions, scalable to large neural networks, and efficient in reducing the number of system states while computing reachable sets. We plan to explore other possibilities for further reducing the over-approximation error, e.g., by using more complex abstract domains such as zonotope.

References

1. Abel, D.: A theory of state abstraction for reinforcement learning. In: Proceedings of the AAAI Conference on Artificial Intelligence. vol. 33, pp. 9876–9877 (2019)
2. Althoff, M.: An introduction to cora 2015. In: Proc. of the workshop on applied verification for continuous and hybrid systems. pp. 120–151 (2015)
3. Althoff, M., Frehse, G., Girard, A.: Set propagation techniques for reachability analysis. *Annual Review of Control, Robotics, and Autonomous Systems* **4**(1) (2021)
4. Althoff, M., Magdici, S.: Set-based prediction of traffic participants on arbitrary road networks. *IEEE Transactions on Intelligent Vehicles* **1**(2), 187–202 (2016)
5. Alur, R., Courcoubetis, C., Halbwachs, N., Henzinger, T.A., Ho, P.H., Nicollin, X., Olivero, A., Sifakis, J., Yovine, S.: The algorithmic analysis of hybrid systems. *Theoretical computer science* **138**(1), 3–34 (1995)
6. Asarin, E., Mysore, V.P., Pnueli, A., Schneider, G.: Low dimensional hybrid systems—decidable, undecidable, don’t know. *Information and Computation* **211**, 138–159 (2012)
7. Bertsekas, D.P., Rhodes, I.B.: On the minimax reachability of target sets and target tubes. *Automatica* **7**(2), 233–247 (1971)
8. Chen, X., Abraham, E., Sankaranarayanan, S.: Taylor model flowpipe construction for non-linear hybrid systems. In: 2012 IEEE 33rd Real-Time Systems Symposium. pp. 183–192. IEEE (2012)
9. Chen, X., Ábrahám, E., Sankaranarayanan, S.: Flow*: An analyzer for non-linear hybrid systems. In: International Conference on Computer Aided Verification. pp. 258–263. Springer (2013)
10. Dutta, S., Chen, X., Sankaranarayanan, S.: Reachability analysis for neural feedback systems using regressive polynomial rule inference. In: Proceedings of the 22nd ACM International Conference on Hybrid Systems: Computation and Control. pp. 157–168 (2019)
11. Fan, F.L., Xiong, J., Li, M., Wang, G.: On interpretability of artificial neural networks: A survey. *IEEE Transactions on Radiation and Plasma Medical Sciences* **5**(6), 741–760 (2021)
12. Fan, J., Huang, C., Chen, X., Li, W., Zhu, Q.: Reachnn*: A tool for reachability analysis of neural-network controlled systems. In: International Symposium on Automated Technology for Verification and Analysis. pp. 537–542. Springer (2020)
13. Frehse, G., Guernic, C.L., Donzé, A., Cotton, S., Ray, R., Lebeltel, O., Ripado, R., Girard, A., Dang, T., Maler, O.: Spaceex: Scalable verification of hybrid systems. In: International Conference on Computer Aided Verification. pp. 379–395. Springer (2011)
14. Gallestey, E., Hokayem, P.: Lecture notes in nonlinear systems and control (2019)
15. Gomes, L.: When will google’s self-driving car really be ready? it depends on where you live and what you mean by" ready"[news]. *IEEE Spectrum* **53**(5), 13–14 (2016)
16. Huang, C., Fan, J., Li, W., Chen, X., Zhu, Q.: Reachnn: Reachability analysis of neural-network controlled systems. *ACM Transactions on Embedded Computing Systems (TECS)* **18**(5s), 1–22 (2019)
17. Ivanov, R., Carpenter, T., Weimer, J., Alur, R., Pappas, G., Lee, I.: Verisig 2.0: Verification of neural network controllers using taylor model preconditioning. In: International Conference on Computer Aided Verification. pp. 249–262. Springer (2021)
18. Ivanov, R., Carpenter, T.J., Weimer, J., Alur, R., Pappas, G.J., Lee, I.: Verifying the safety of autonomous systems with neural network controllers. *ACM Transactions on Embedded Computing Systems (TECS)* **20**(1), 1–26 (2020)
19. Jin, P., Tian, J., Zhi, D., Wen, X., Zhang, M.: : A cegar-driven training and verification framework for safe deep reinforcement learning. In: International Conference on Computer Aided Verification. pp. 193–218. Springer (2022)

20. Limon, D., Bravo, J., Alamo, T., Camacho, E.: Robust mpc of constrained nonlinear systems based on interval arithmetic. *IEE Proceedings-Control Theory and Applications* **152**(3), 325–332 (2005)
21. Lygeros, J., Tomlin, C., Sastry, S.: Controllers for reachability specifications for hybrid systems. *Automatica* **35**(3), 349–370 (1999)
22. Park, S., Kim, J., Kim, G.: Time discretization-invariant safe action repetition for policy gradient methods. *Advances in Neural Information Processing Systems* **34**, 267–279 (2021)
23. Pereira, A., Althoff, M.: Overapproximative human arm occupancy prediction for collision avoidance. *IEEE Transactions on Automation Science and Engineering* **15**(2), 818–831 (2017)
24. Runger, M., Tabuada, P.: Computing robust controlled invariant sets of linear systems. *IEEE Transactions on Automatic Control* **62**(7), 3665–3670 (2017)
25. Schilling, C., Forets, M., Guadalupe, S.: Verification of neural-network control systems by integrating taylor models and zonotopes. In: *Proceedings of the AAAI Conference on Artificial Intelligence*. vol. 36, pp. 8169–8177 (2022)
26. Schmidt, L.M., Kontes, G., Plinge, A., Mutschler, C.: Can you trust your autonomous car? interpretable and verifiably safe reinforcement learning. In: *2021 IEEE Intelligent Vehicles Symposium (IV)*. pp. 171–178. IEEE (2021)
27. Schürmann, B., Kochdumper, N., Althoff, M.: Reachset model predictive control for disturbed nonlinear systems. In: *2018 IEEE Conference on Decision and Control (CDC)*. pp. 3463–3470. IEEE (2018)
28. Scott, J.K., Raimondo, D.M., Marseglia, G.R., Braatz, R.D.: Constrained zonotopes: A new tool for set-based estimation and fault detection. *Automatica* **69**, 126–136 (2016)
29. Shalev-Shwartz, S., Shammah, S., Shashua, A.: Safe, multi-agent, reinforcement learning for autonomous driving. *arXiv preprint arXiv:1610.03295* (2016)
30. Su, J., Chen, W.H.: Model-based fault diagnosis system verification using reachability analysis. *IEEE Transactions on Systems, Man, and Cybernetics: Systems* **49**(4), 742–751 (2017)
31. Szegedy, C., Zaremba, W., Sutskever, I., Bruna, J., Erhan, D., Goodfellow, I., Fergus, R.: Intriguing properties of neural networks. In: *2nd International Conference on Learning Representations, ICLR 2014* (2014)
32. Tran, H.D., Bak, S., Xiang, W., Johnson, T.T.: Verification of deep convolutional neural networks using imagestars. In: *International conference on computer aided verification*. pp. 18–42. Springer (2020)
33. Tran, H.D., Cai, F., Diego, M.L., Musau, P., Johnson, T.T., Koutsoukos, X.: Safety verification of cyber-physical systems with reinforcement learning control. *ACM Transactions on Embedded Computing Systems (TECS)* **18**(5s), 1–22 (2019)
34. Tran, H.D., Yang, X., Manzananas Lopez, D., Musau, P., Nguyen, L.V., Xiang, W., Bak, S., Johnson, T.T.: Nnv: the neural network verification tool for deep neural networks and learning-enabled cyber-physical systems. In: *International Conference on Computer Aided Verification*. pp. 3–17. Springer (2020)
35. Virtanen, P., Gommers, R., Oliphant, T.E., et al.: SciPy 1.0: Fundamental Algorithms for Scientific Computing in Python. *Nature Methods* **17**, 261–272 (2020)
36. Xue, B., Easwaran, A., Cho, N.J., Fränzle, M.: Reach-avoid verification for nonlinear systems based on boundary analysis. *IEEE Transactions on Automatic Control* **62**(7), 3518–3523 (2016)
37. Yampolskiy, R.V.: Unexplainability and incomprehensibility of ai. *Journal of Artificial Intelligence and Consciousness* **7**(02), 277–291 (2020)

A Assessing Verisig 2.0 with Big Weights

Verisig 2.0 may fail to verify the reach-avoid problems when dealing with neural networks with big weights. To demonstrate this, we initialize the weights of neural network with larger values (random numbers $w_l \sim \mathcal{N}(\mu, \sigma^2)$ with $\mu = 0, \sigma = 0.1$) and show the experimental results in Figure 10. We observe that the calculated reachable sets contain large over-approximation error except for B4. In Tora, Verisig 2.0 fails to calculate the complete reachable sets due to too large over-approximation error. Hence, it is fairly to say that Verisig 2.0 is sensitive to big weights.

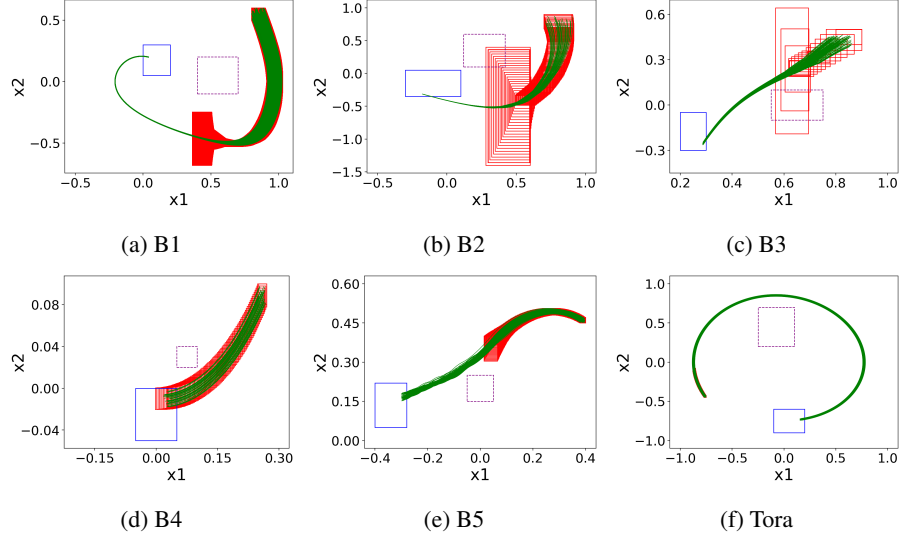


Fig. 10: Assessing Verisig 2.0 on Larger Networks with Big Weights. Red box: reachable set; Green lines: simulation trajectories; Blue box: goal region; Purple dashed box: unsafe region.

B Benchmarks Setting

We provide the setting of seven benchmarks in Table 2. The initial region and goal region are the same as the setting in [17]. The abstraction granularity is a hyper-parameter used in the abstraction-based training and the calculation of reachable sets. All the experimental results in Section 5.2 and Section 5.3 are based on the following settings.

C Tightness Comparison

This section presents the tightness comparison results on B3, B4, B5 and ACC in Figure 11. For B3, B4 and B5, all methods achieve similar results. However, for ACC,

Table 2: Benchmarks Setting

Task	Abstraction Granularity	Initial Region	Goal Region	Unsafe Region
B1	[0.02, 0.02]	$x_1 \in [0.8, 0.9]$ $x_2 \in [0.5, 0.6]$	$x_1 \in [0, 0.2]$ $x_2 \in [0.05, 0.3]$	$x_1 \in [0.4, 0.7]$ $x_2 \in [-0.1, 0.2]$
B2	[0.1, 0.1]	$x_1 \in [0.7, 0.9]$ $x_2 \in [0.7, 0.9]$	$x_1 \in [-0.3, 0.1]$ $x_2 \in [-0.35, 0.5]$	$x_1 \in [0.12, 0.42]$ $x_2 \in [0.1, 0.6]$
B3	[0.2, 0.2]	$x_1 \in [0.8, 0.9]$ $x_2 \in [0.4, 0.5]$	$x_1 \in [0.2, 0.3]$ $x_2 \in [-0.3, -0.05]$	$x_1 \in [0.55, 0.75]$ $x_2 \in [-0.1, 0.1]$
B4	[0.2, 0.2, 0.2]	$x_1 \in [0.25, 0.27]$ $x_2 \in [0.08, 0.1]$ $x_3 \in [0.25, 0.27]$	$x_1 \in [-0.05, 0.05]$ $x_2 \in [-0.05, 0]$	$x_1 \in [0.05, 0.1]$ $x_2 \in [0.02, 0.04]$
B5	[0.1, 0.1, 0.1]	$x_1 \in [0.38, 0.4]$ $x_2 \in [0.45, 0.47]$ $x_3 \in [0.25, 0.27]$	$x_1 \in [-0.4, -0.28]$ $x_2 \in [0.05, 0.22]$	$x_1 \in [-0.05, 0.05]$ $x_2 \in [0.15, 0.25]$
Tora	[0.2, 0.2, 0.2, 0.2]	$x_1 \in [-0.77, -0.75]$ $x_2 \in [-0.45, -0.43]$ $x_3 \in [0.51, 0.54]$ $x_4 \in [-0.3, -0.28]$	$x_1 \in [-0.1, 0.2]$ $x_2 \in [-0.9, -0.6]$	$x_1 \in [-0.25, 0.10]$ $x_2 \in [0.2, 0.7]$
ACC	[1, 0.1, 0.1, 1, 0.1, 0.1]	$x_1 \in [90, 91]$ $x_2 \in [32, 32.05]$ $x_4 \in [10, 11]$ $x_5 \in [30, 30.05]$ $x_3, x_6 \in [0, 0]$	$x_2 \in [22.81, 22.87]$ $x_5 \in [29.88, 30.02]$	$x_2 \in [26, 29]$ $x_5 \in [30.05, 30.15]$

a 6-dimensional environment, the sample-based approach ReachNN* produces huge over-approximation error.

D Differential and Decomposing Analysis Results

In this section, we provide the complete differential and decomposing analysis results in Figure 12 and Figure 13. All of these results are consistent with the conclusion in Section 5.4.

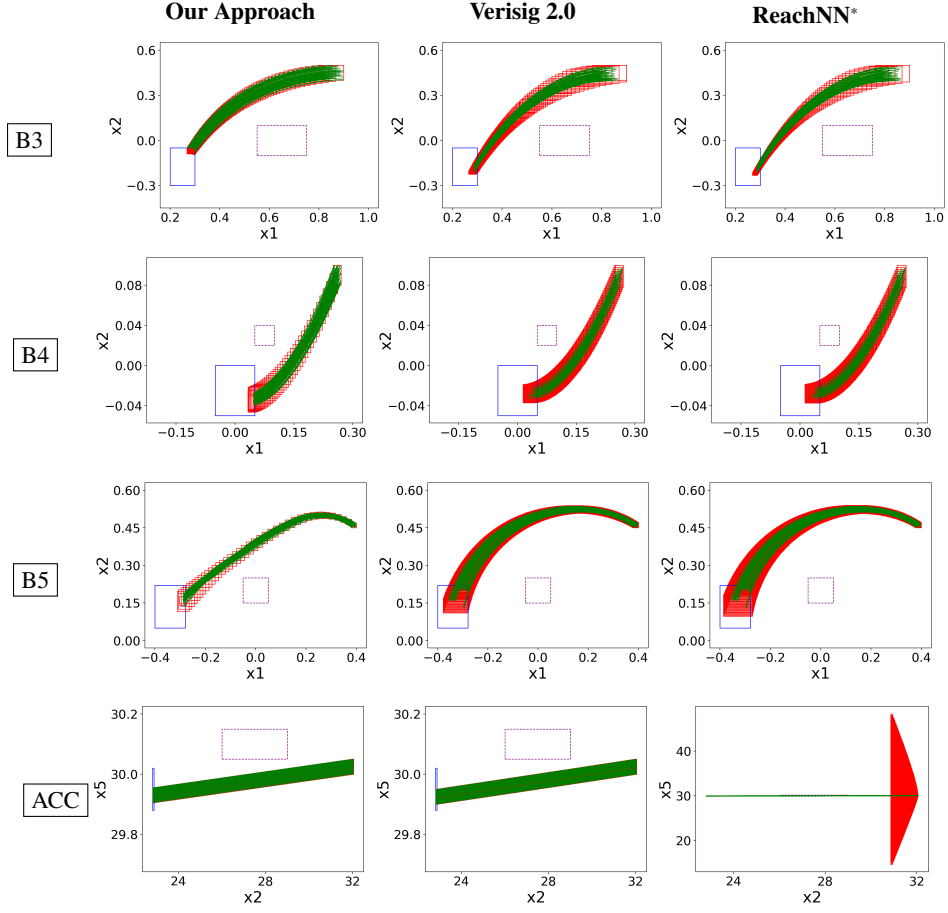


Fig. 11: Larger network with Tanh activation function. Red box: reachable set; Green lines: simulation trajectories; Blue box: goal region; Purple dashed box: unsafe region.

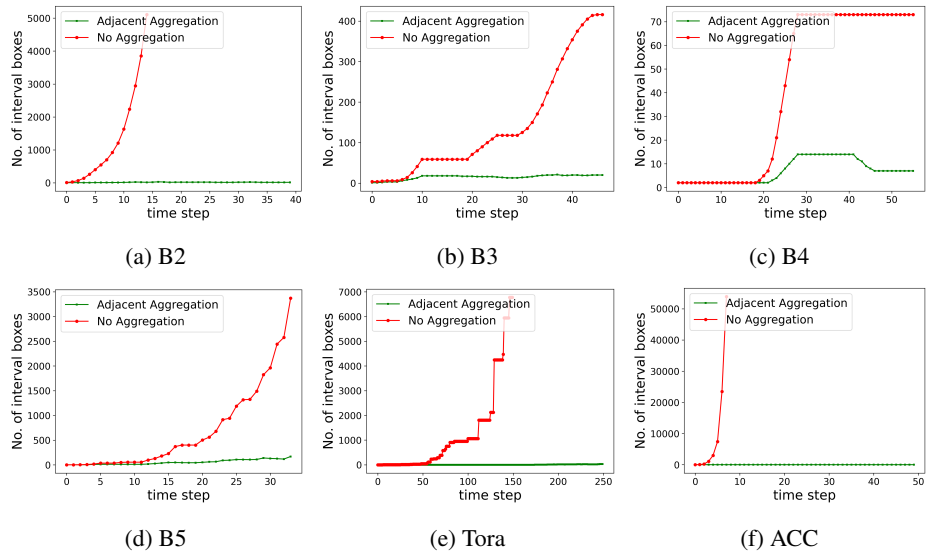


Fig. 12: Differential Analysis Results.

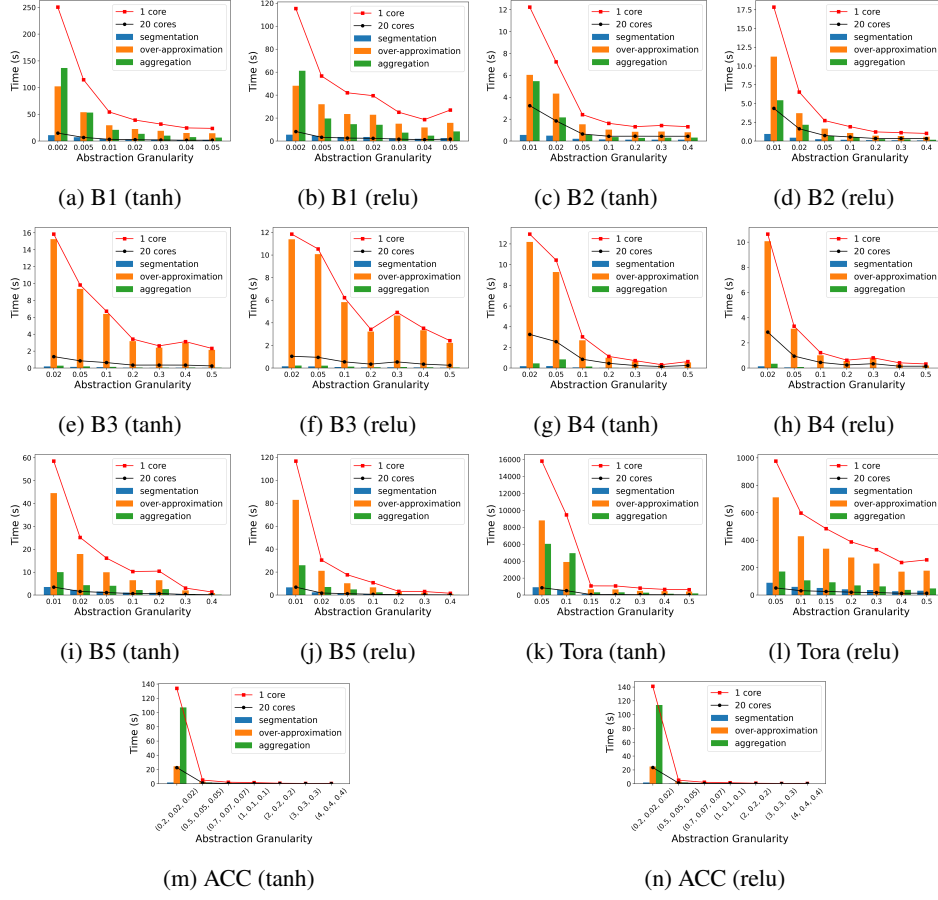


Fig. 13: Decomposing Analysis Results. Due to the space reason, for B1-B5 and Tora, we use a scalar value x_1 to denote the n -dimensional abstraction granularity vector $\gamma = (x_1, \dots, x_1)$. For ACC, we use a 3-dimensional vector (x_1, x_2, x_3) to denote the 6-dimensional abstraction granularity vector $\gamma = (x_1, x_2, x_3, x_1, x_2, x_3)$